Passive discrete lens for broadband elastic guided wave focusing

Emeline Sadoulet-Reboul, Gaël Matten, Kaijun Yi, Morvan Ouisse

OVERLAY

Journal of Theoretical, Computational and Applied Mechanics

JTCAM

DIAMOND OPEN ACCESS

Passive discrete lens for broadband elastic guided wave focusing

Emeline Sadoulet-Reboul[1,*] , **Gaël Matten**[1] , **Kaijun Yi**[2] , **Morvan Ouisse**[1]

[1] Univ. Bourgogne Franche-Comté - FEMTO-ST Institute, Department of Applied Mechanics, 24, rue de l'Epitaphe, 25000 Besancon, France

[2] School of Aerospace Engineering, Beijing Institute of Technology, Beijing 100081, PR China

[*] Corresponding author: Emeline.Sadoulet-Reboul@univ-fcomte.fr

Elastic guided wave focusing is of great interest for applications such as vibroacoustic control, energy harvesting, or Structural Health Monitoring. Different strategies allow generation of this effect, GRadient-INdex devices in particular exploit medium with varying properties such as thickness to reproduce an adequate refractive index profile as in optics. The resulting continuous profiles have a curved geometry that can be hard to manufacture, and be difficult to integrate in a given design. The purpose of this paper is to propose a discrete design for a GRIN lens. It is composed of segments selected in number and thickness to give similar focusing effects as a continuous lens profile. The identified configuration is manufactured and bounded on an aluminium plate to evaluate the effective focusing performances. Numerical and experimental vibrometry results confirm that the proposed lens exhibits a fixed focal point over a broad frequency range. The discrete design overcomes fabrication issues encountered in continuous design, allowing for an easier integration in devices for elastic wave control.

Keywords GRIN Lens, Wave control, Elastic waves, Refractive index

1 Introduction

Focusing of elastic waves is of high interest for applications such as energy harvesting (Carrara et al., 2012, Tol et al., 2016, Hyun et al., 2019), Structural Health Monitoring (Kudela et al., 2018), or acoustic imaging (Davis et al., 2007, Deng et al., 2009, Peng et al., 2010). Indeed, by concentrating the propagating waves at an identified focal point it is possible to extract more energy, to enhance the efficiency of harvesters, to aliment small wearable autonomous devices, to spatially localize wave informations, or again to increase imaging resolution and accuracy. Different strategies have emerged to achieve wave control such as Phononic crystals (PC) consisting

in periodic structures exhibiting phononic bandgaps (Timorian et al., 2020), Elastic MetaMaterials (EMMs) that exploit local resonances (Campana et al., 2020), acoustic mirrors based on specific parabolic or elliptic shapes to generate curved trajectories and localize elastic waves (Carrara et al., 2012), or continuous profile (Krylov and Tilman, 2004). All these solutions can be used to give rise to GRadient-INdex devices (GRIN): their purpose is to reproduce the inhomogeneous behavior of materials in which propagating waves follow curved trajectories under adequate refractive properties as observed in optics (Gomez-Reino et al., 2012). The focus of elastic waves is realized by controlling the variations of the index of refraction or wave velocity along the axis transverse to the direction of propagation.

Gradient-Index Phononic Crystals (PC) consist of scatterers, typically inclusions as air holes or metallic inclusions, placed in an elastic matrix (silicone for instance). The acoustic velocity gradient adequate to generate the refractive index is obtained by changing the holes or inclusions radii (Sukhovich et al., 2008, Wu et al., 2011, Zhao et al., 2012), the lattice spacing (Centeno and Cassagne, 2005, Kurt et al., 2008, Peng et al., 2010), or changing the elastic properties of the inclusions (Lin et al., 2009). Elastic Metamaterials (EMMs) exploit local resonances in periodic structures instead of multiple scattering, the GRIN-lens consists, in this case, of a set of solid cylinders or pillars (Yan et al., 2013) : the phase velocity is modified by spatially changing the elastic properties like the mass density profile, or similarly the thicknesses, the material or geometrical properties. Advances in additive manufacturing techniques give emergence of 3D-printed Gradient-Index Lenses (Tol et al., 2019). While PC or EMM-based flat lenses exhibit negative refraction properties within quite narrow frequency band due to the principle linked to the dispersion bands of the structures, GRIN-based configurations allow to focus waves on larger bandwidths (Lin et al., 2009). Recent studies have shown that two-dimensional periodic lattices of Acoustic Black Holes (ABH) allow a focusing effect to be achieved on a broadband frequency band that spans the metamaterial and the phononic range (Zhu and Semperlotti, 2017). Another strategy to focus waves consists in using acoustic mirrors with elliptical or parabolic geometries: the first developments did consist of stub extensions (Carrara et al., 2012, 2013, 2015) and it has been shown more recently that it was possible to improve the mirror efficiency defining a geometry-wavelength design criterion, and that the harvested power could be drastically increased using a structurally embedded mirror based on metallic spheres inserted into blind holes (Tol et al., 2017). The refractive index can also be controlled using continuously varying profiles, and changing typically the thickness or similarly the rigidity of the main structure (Krylov and Tilman, 2004, Georgiev et al., 2011, Climente et al., 2014, Zareei et al., 2018) : such approaches exploit the thickness-dependence of the dispersion relation of flexural waves to create an adequate gradient index. Besides, by coupling the strategies as varying simultaneously the filling fraction of a Phononic Crystal Lens and the thickness of the plate it seems possible to control not only the lowest-order antisymmetric Lamb Mode (A_0) in a plate as classically done, but to consider broadband multimodal control focusing on the two lower order Lamb Modes (A_0 and S_0) (Jin et al., 2015). Finally, semi-active, active or adaptive strategies utilize multiphysic coupling such as electromechanical or thermomechanical to control wave propagation (Yi et al., 2019, Billon et al., 2019), and have allow to develop lenses for wave focusing (Chiou et al., 2014, Yi et al., 2016, Xu et al., 2017).

Despite the development of innovative and more effective manufacturing techniques, most of the solutions presented previously are difficult to fabricate. Active solutions require to control complex and potentially sensitive multiphysical couplings. Passive solutions require precision at small scales for many unit cells, or the required curved shape for continuous profile are complex for conventional machining centres and generate a lot of manufacturing issues. The purpose of this paper is to propose a design for a passive discrete lens simpler to manufacture and that allows good focusing effect on a large frequency band. The discrete configuration is obtained from a preliminary study done on a continous curved profile and consists in the discretization of the continuous profile into a limited number of segments. Numerical simulations and experimental results converge to show that only few segments are necessary to guide and focus waves effectively in a specific area. The passive discrete lens allows more flexibility in terms of fabrication, and does not require complex manufacturing tools. The paper is organized as follows. the design of a passive lens based on a continuous curved profile is presented in section 2. This profile is used as a reference to propose a discrete configuration as investigated in section 3. The obtained

GRIN lens is manufactured and experimental results obtained through vibrometry measurements are compared to numerical simulations to validate the proposed design and confirm the focusing performances in section 4. Finally, some comments and perspectives are given in the concluding section.

2 Design of a passive GRadient-Index lens based on a continuous curved profile

A GRadient-INdex lens aims at reproducing by a gradient the refractive index of a material. An index of refraction with an hyperbolic secant variation in the direction perpendicular to the waves' propagation direction is known to be capable of focusing waves without aberration (Lin et al., 2009). Let consider a rectangular plate with principal direction x and in-plane perpendicular direction y (Fig. 1a), the refractive index is written as,

$$n(y) = n_0 \sec(\alpha(y - \beta)) \tag{1}$$

where n_0 is the refractive index at lens' core (x-axis, $y = \beta$) and α is the gradient coefficient (Fig. 1b).

This coefficient is linked to the focal length f_l by the relation,

$$f_l = \frac{\pi}{2\alpha}. \tag{2}$$

For the reference case detailed in this section, the gradient is obtained by varying the thickness of a thin plate where elastic wave focusing is expected (Zareei et al., 2018). The propagation of flexural waves in a thin plate modeled as a Kirchhoff-Love plate is described by a fourth-order partial differential equation (Eq. (3)),

$$D\nabla^4 w + \rho h \frac{\partial^2 w}{\partial t^2} = 0. \tag{3}$$

w is the transverse displacement of the plate, $D = Eh^3/12\rho\left(1-\nu^2\right)$ denotes the flexural rigidity of the plate, E is the Young modulus, ν the Poisson'ratio, ρ the density and h the thickness of the plate. For a harmonic wave propagation, the dispersion relation that links the wavenumber k to the angular frequency ω for flexural waves can be written as,

$$Dk^4 = \rho h_b \omega^2, \tag{4}$$

and thus the phase velocity c is

$$c^4 = \frac{k^4}{\omega^4} = \frac{Eh^2\omega^2}{12\rho\left(1-\nu^2\right)}. \tag{5}$$

Referring to optics, the refractive index n is defined as the ratio of the velocity c_0 of the waves in the homogenous plate with initial fixed thickness h_0 to their velocity c in the lens with varying thickness h,

$$n(y) = \frac{c_0}{c(y)}. \tag{6}$$

If the lens material is the same as the plate material and doesn't depend on space, the gradient of the refractive index is directly linked to the gradient of the thickness,

$$n(y) = \sqrt{\frac{h_0}{h(y)}} \tag{7}$$

$$h(y) = h_0 \cos^2\left[\alpha(y - \beta)\right]. \tag{8}$$

As this relation doesn't depend on the angular frequency, it is valid for any excitation frequency and thus a focusing effect on a wide frequency band can be expected.

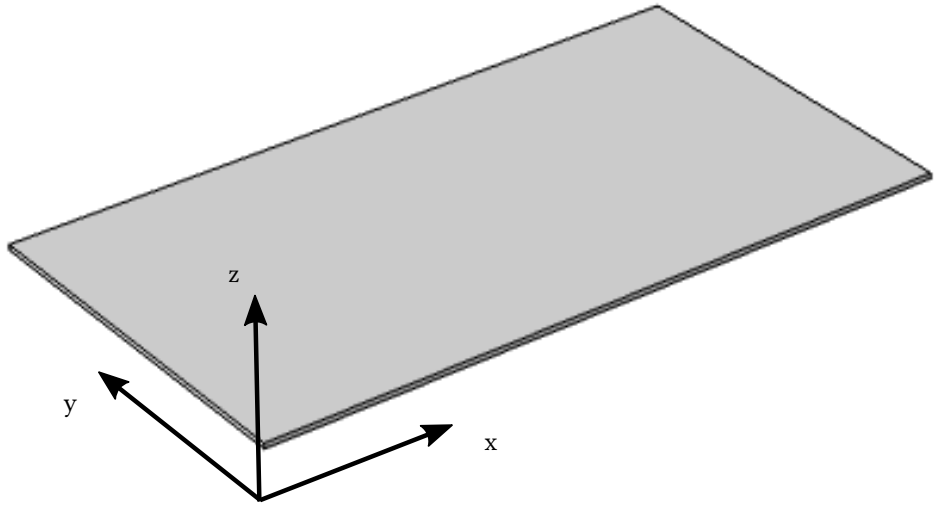

(a) Plate orientation axes

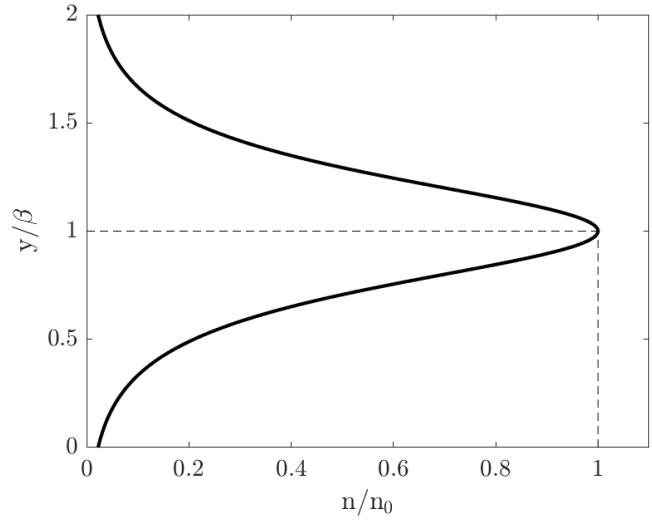

(b) Refractive index defined as a hyperbolic secant function with n_0 at lens' core, and β at the focal point

Fig. 1: Orientation axes and refractive index

2.1 Case of a symmetrical GRIN lens

For the first application case the GRIN lens is designed to be symmetrical to the mid-plane of the thin plate considering the symmetry of the propagating medium : Fig.2 shows the evolution of the thickness of the lens to generate the refractive profile proposed in Eq. (8). The host plate is 5 mm thick and the gradient coefficient α is chosen for the focal length to be equal to 0.35 cm. All the parameters for the studies are recalled in A.
The FE method is used to simulate the wave propagation in a plate incorporating the symmetrical GRIN lens. The

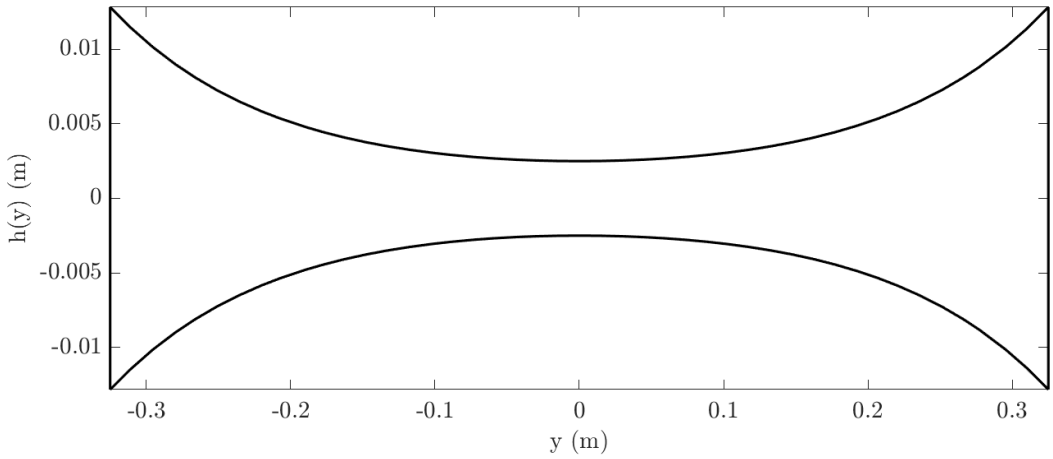

Figure 2: Profile of the symmetrical GRIN lens

length of the plate is 1.9 m, its width is 0.65 m. It is made of aluminium with properties E=70 Gpa for the Young's modulus, ν = 0.3 for the Poisson's ratio, ρ = 2700 kg.m^3 for the density. In order to excite the structure, a plane wave front is generated by an array of 18 piezoelectric transducers (PIC 151, 3 cm $\times$ 3 cm $\times$ 0.5 mm) bonded to the aluminium plate with equal spacing (around 6.5 mm). A Perfectly Matched Layer (PML) is introduced at the boundary of the plate to absorb outgoing waves, simulating an infinite plate and minimizing reflections. Fig. 3 presents the full problem studied as well as the Finite Element mesh used for the study. It is composed of quadratic brick elements that were necessary for the electromechanical simulation despite the thin thicknesses involved. The maximum element length is chosen to ensure 8 mesh elements per wavelength, and a distribution of two elements in the thickness is imposed. A multiphysic frequency domain simulation is performed in order to solve simultaneously the electrostatics and the solid mechanics equations for different frequencies, 2350 Hz, 3450 Hz, 4400 Hz, 5300 Hz, 6850 Hz and 7900 Hz. The nondimensionalized transverse velocity fields obtained are presented in Fig.4. The maximum field value in each of the computational areas is used to adimensionalize the results. It can be observed that, as expected, waves join the focal point indicated by a magenta cross, and then propagate in the main direction of the plate.
It can be observed from numerical simulations that the focusing effect is always visible at the expected focal point for all the frequencies.

2.2 Case of a unsymmetrical GRIN lens

One major difficulty with the symmetrical GRIN lens is the needed space as both sides of the plate are covered. For this reason a second application case is considered to investigate the focus efficiency that can be obtained with an unsymmetrical GRIN lens. The new profile is presented on figure 5.
Same simulations as for the symmetrical lens are done and the results obtained for the different frequencies are presented on figure 6.
The focusing effect still appears on the whole frequency band, even if it is more pronounced for higher frequencies.

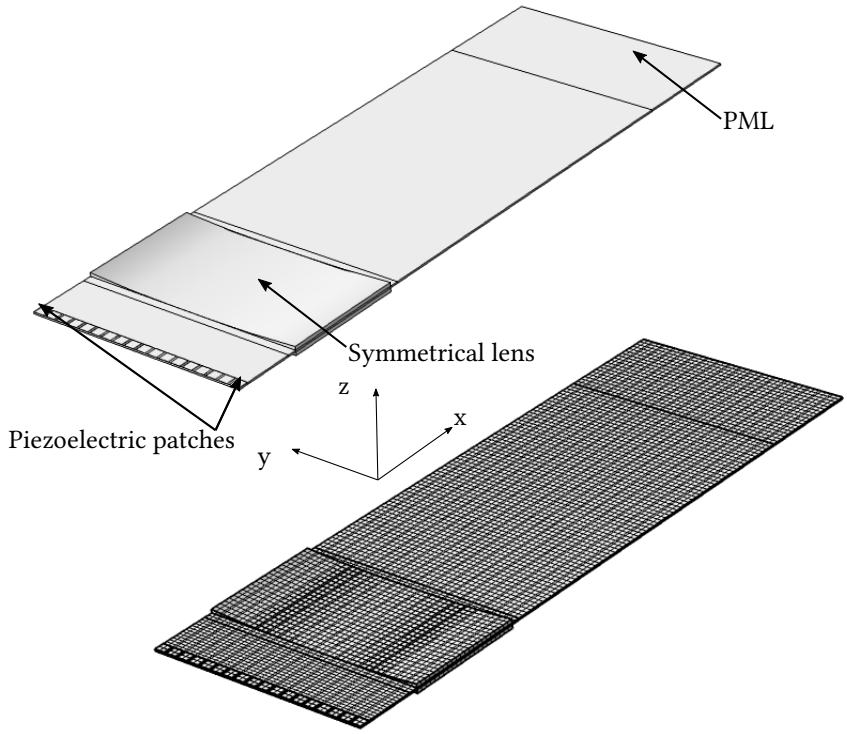

Figure 3: Integration of the symmetrical GRIN lens in the plate to focus transversal waves - Piezolectric patches are used to generate an incident plane wave front, and a Perfectly Matched Layer (PML) is introduced at the boundary to avoid reflections. FE mesh

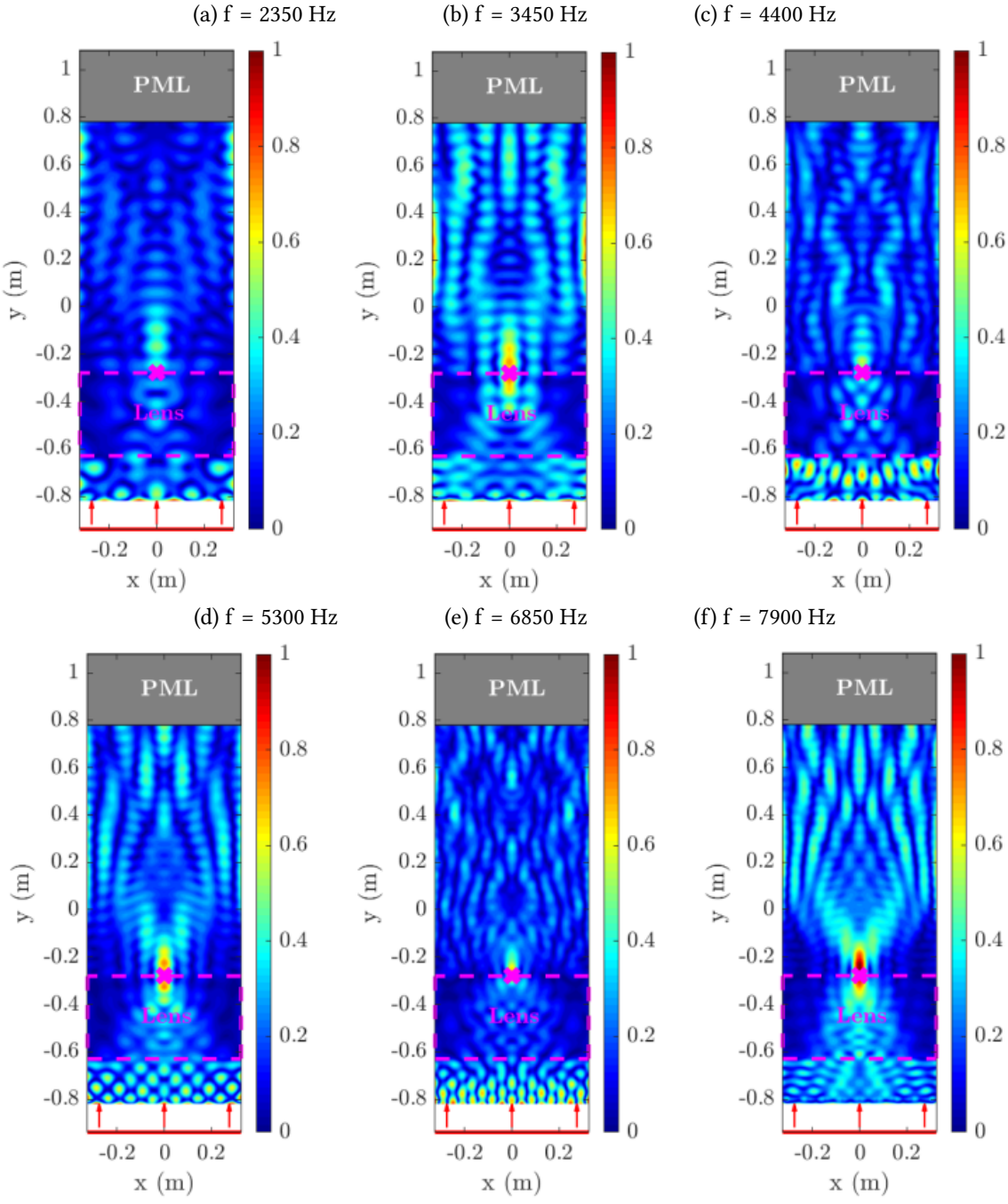

Figure 4: Nondimensionalized transverse velocity amplitude for different excitation frequencies computed with a symmetrical continuous lens : (a) 2350 Hz, (b) 3450 Hz, (c) 4400 Hz, (d) 5300 Hz, (e) 6850 Hz, (f) 7900 Hz

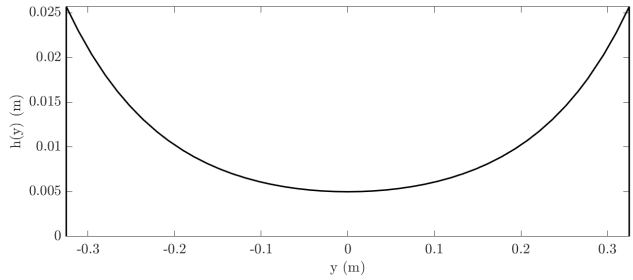

Figure 5: Profile of the unsymmetrical GRIN lens

3 Design of a passive GRadient-Index lens based on a discrete curved profile

The previous section has shown that it is possible to obtained good focusing effects on a large frequency band using an unsymmetrical GRadient-Index lens. Despite the unilateral design, the continuous curved profile remains difficult to manufacture which can be an obstacle for industrial applications. For this reason it is proposed to study the possibility to obtain similar focusing effects as for the continuous case using a discrete curved profile. Thus, the profile is divided into segments, and three configurations are considered arbitrary fixed to 7, 11 and 15 segments. All segments have the same width and their thicknesses correspond to the average of the thickness values given by the continuous profile at the ends of each segment. Figure 7 presents the associated discrete profiles for the lens.

3.1 Discretization of the curved profile

To estimate an adequate discretization of the curved profile, numerical simulations are performed to compare the amplitude of the quadratic transverse velocity of the plate obtained along the central line in the direction of the plate that crosses the focal point. The symmetrical continuous profile is always used as a reference. Figure 8 presents the obtained results : they are normalized to the maximum value to be comparable. The vertical dot lines indicate the position of the GRIN lens.
It can be observed that the results converge to the reference ones as the number of segments increases, but finally it appears that only 7 segments are enough to obtain good focusing effects. The higher the frequency, the stronger the focusing effect and the more centered in a point it is. Following these conclusions, the proposed unsymmetrical discrete lens is composed of 7 segments with identical widths equal to 92.8 mm and respective thicknesses given in table 1.

4 Validation of the discrete GRIN lens by comparison of experimental and numerical results

In order to perform experiments, the elements composing the lens are manufactured using electroerosion cutting. Due to the symmetry of the lens, two series of three elements with different thicknesses are manufactured, no element is introduced in the center of the lens. They are bonded on a host plate. Figure 9(a) presents the experimental set-up with the aluminium plate mounted on a frame for laser vibrometry measurements, and the

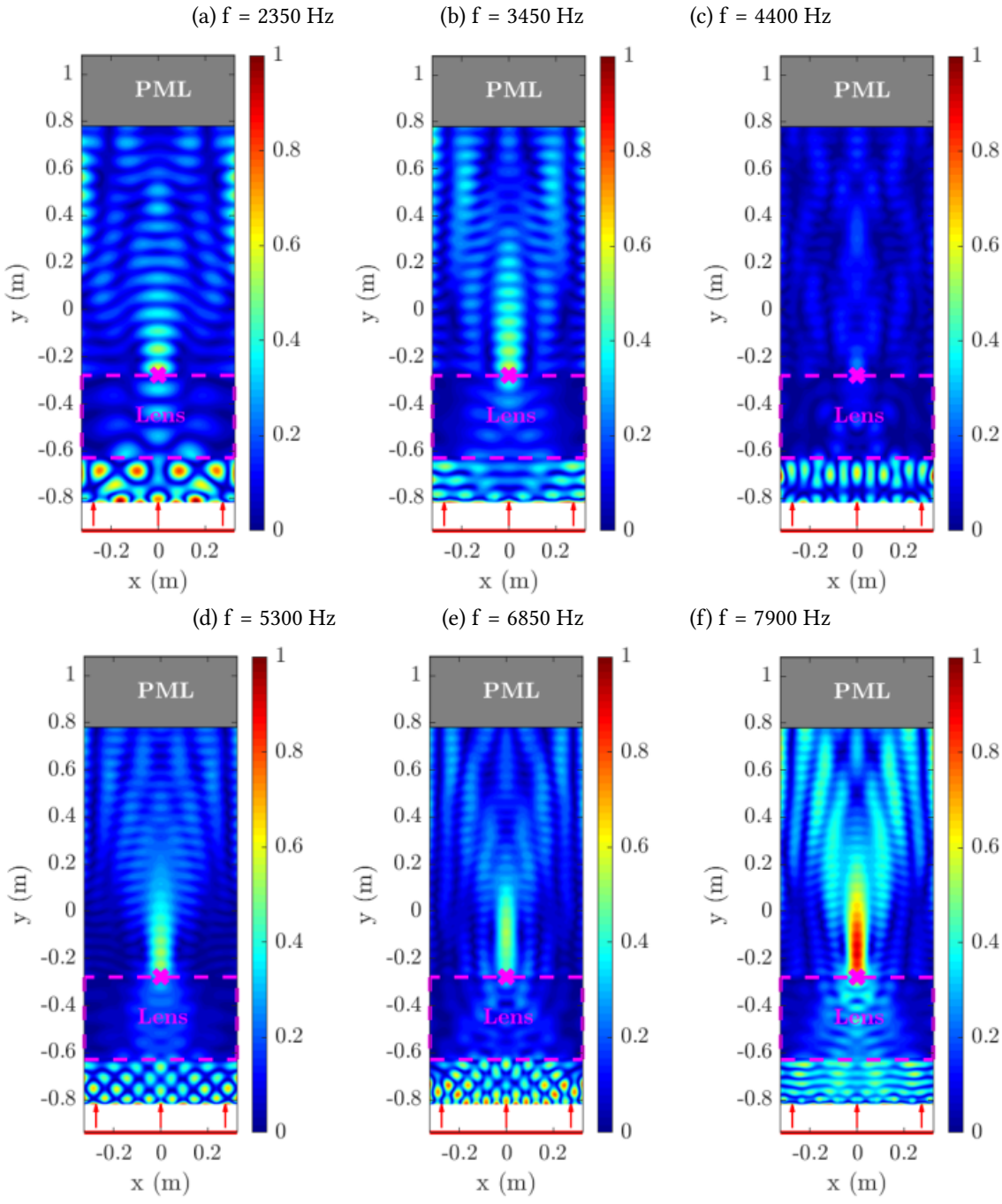

Figure 6: Nondimensionalized transverse velocity amplitude for different excitation frequencies computed with a unsymmetrical continuous lens : (a) 2350 Hz, (b) 3450 Hz, (c) 4400 Hz, (d) 5300 Hz, (e) 6850 Hz, (f) 7900 Hz

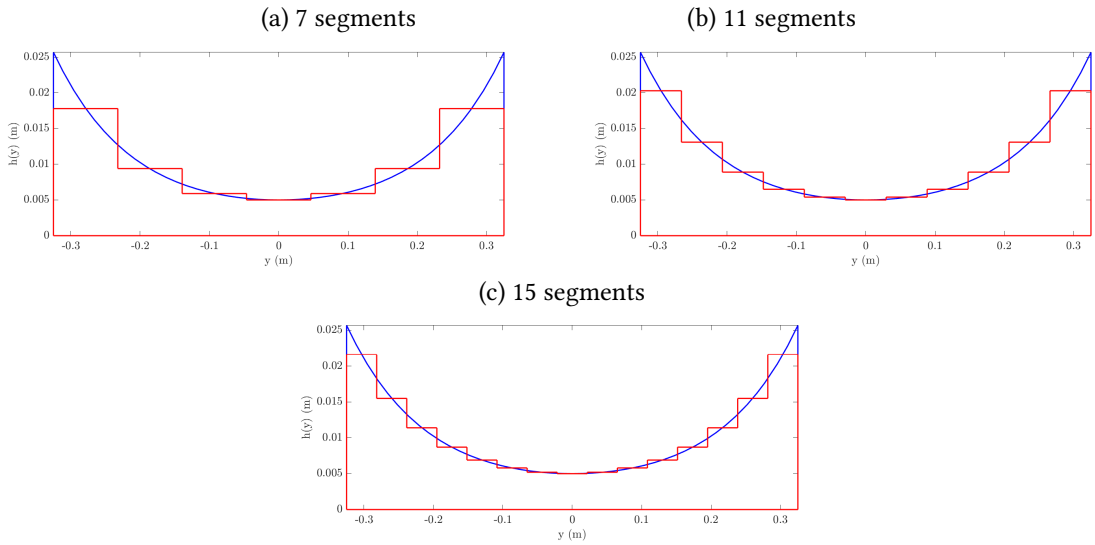

Figure 7: Discretization of the continuours GRIN-lens profile into (a) 7 segments, (b) 11 segments, (c) 15 segments.

Segment	Height [Unit : mm]
Segment 1	12.8
Segment 2	4.4
Segment 3	1.9
Segment 4	0
Segment 5	1.9
Segment 6	4.4
Segment 7	12.8

Table 1: Heights of the 7 segments composing the lens from the left edge to the right edge

bounded GRIN lens (b). The set of 18 piezoelectric transducers used to generate propagative plane waves is visible at the lower edge of the plate. At the top edge a viscoelastic constrained layer is introduced in order to reproduce PML effects, absorb incoming waves and avoid reflections. The layer is made with a 3M VHB polymer, it is 30 cm wide and 3 mm thick, it is constrained thanks to a 1 mm thick aluminium plate: the optimal thickness to ensure the best absorption has been obtained from preliminary numerical simulations.
Wavelets at central frequencies are applied to the transducers using a numerical circuit and a voltage amplifier. The transverse velocity of the plate is measured in the time domain on a grid of points using a Polytec infrared scanning laser vibrometer (PSV 500 X-tra). As previously, the FE method is used to compute the transverse velocity for the case of the GRIN discrete lens. The same set of piezoelectric patches is used to generate a plane wave front, and a PML layer is introduced to prevent reflections. Experimental and numerical studies are here done in the time domain. Field representations are solutions obtained at specific times corresponding to focusing at the expected focal point.
Figures 10, 11 and 12 present snapshots of the amplitudes of the experimental (figures a) and numerical (figures b) adimensionalized transverse velocities as well as a comparison (figures c) between the quadratic velocities on the central line in the direction of wave propagation, for frequencies 2350 Hz (case 1), 3450 Hz (case 2), 4400 Hz (case 3), 5300 Hz (case 4), 6850 Hz (case 5), and 7900 Hz (case 6). The domain chosen for the comparison

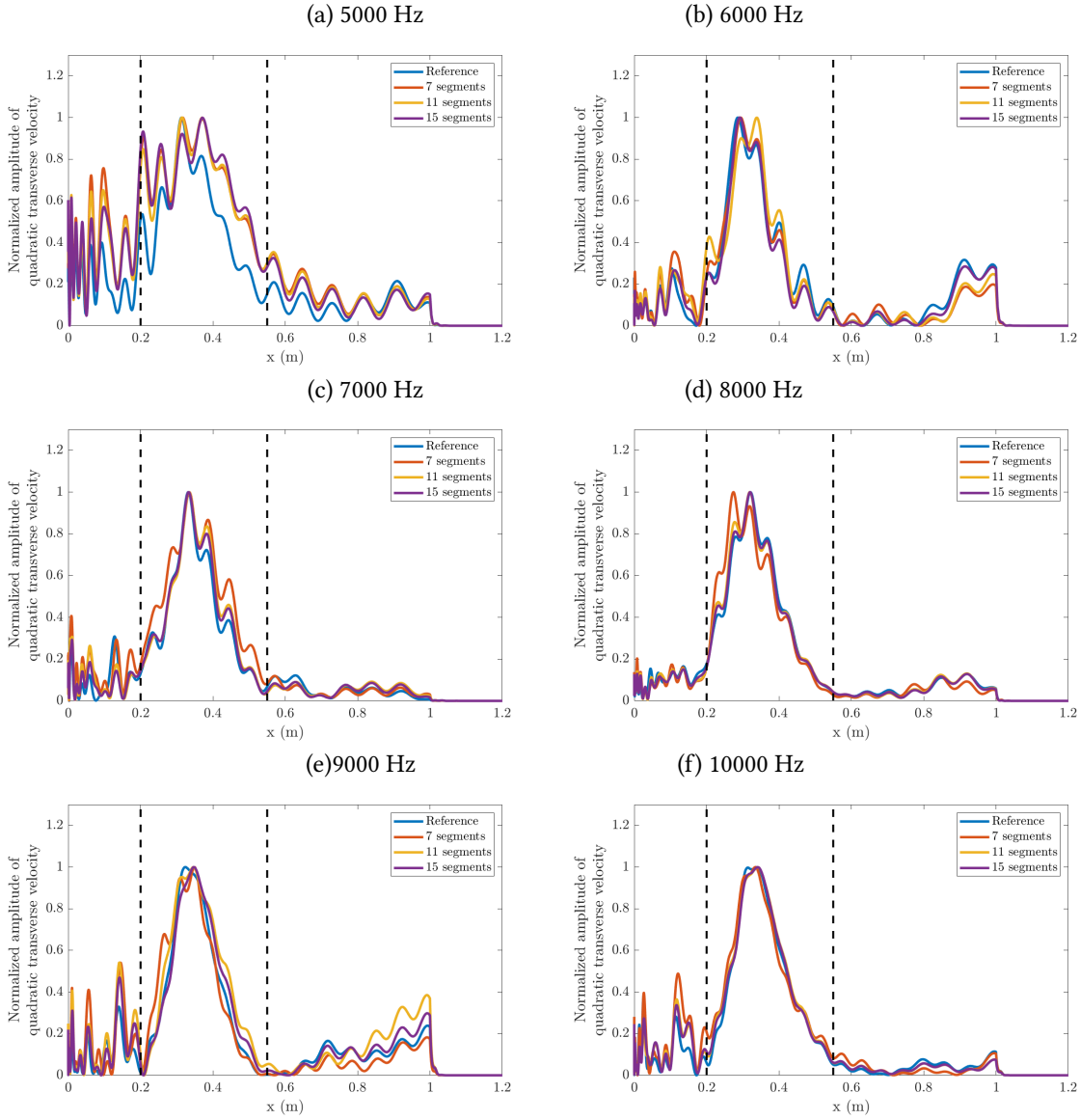

Figure 8: Evolution of the nondimensionalized quadratic transverse velocity along the central line in the direction of the plate for different frequencies between 5000 Hz (case a) to 1000 Hz (case f)

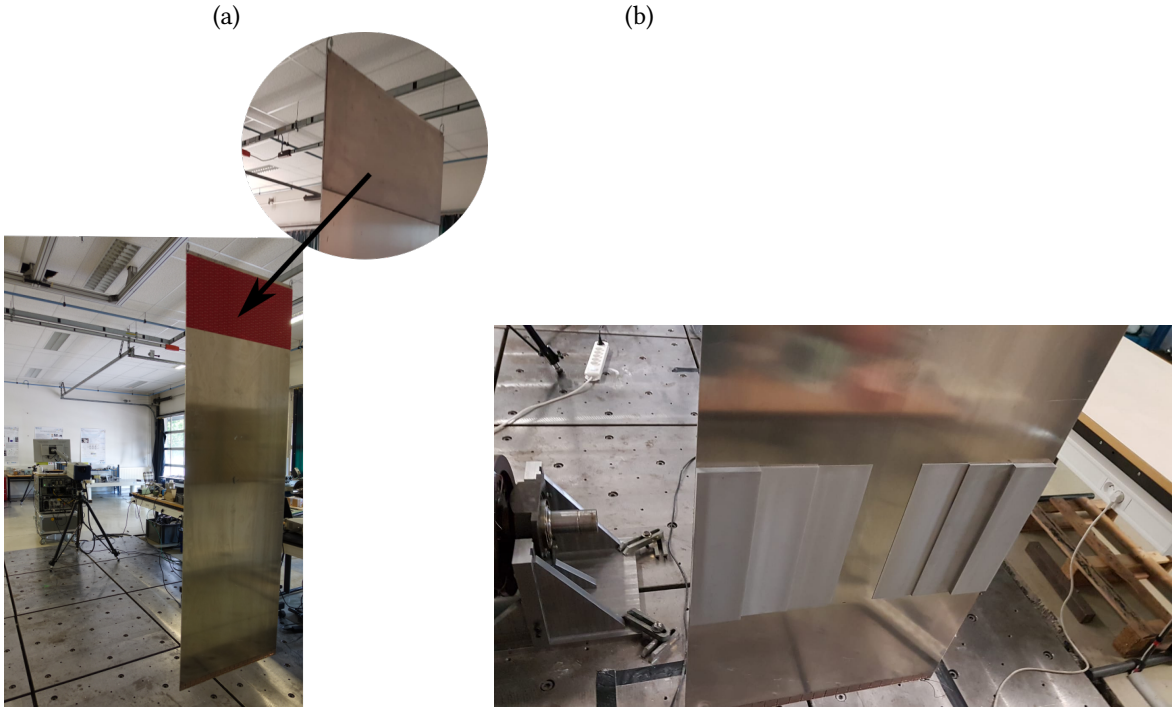

Figure 9: Experimental setup (a) nude plate suspended to a frame, with piezoelectric patches at the lower edge and a constrained viscoelastic layer at the top edge (b) View of the discrete GRIN lens bonded on the plate

between results is set behind the lens. Numerical and experimental results are in good agreement, they confirm the existence of a similar focal point for all the studied frequencies where the wave energy concentrates. This concentration is all the more focalized that frequencies are high, but it is noticeable that the effect is visible for all the studied frequencies.

5 Conclusion

The paper proposes a design for a passive discrete GRIN lens to focus elastic waves. The discrete configuration consists in a set of segments with varying thicknesses in order to generate a refractive index for wave focusing. Numerical simulations done on different discrete configurations and compared to a continuous reference profile show that a reduced number of segments is enough to obtain good focusing effects. The designed GRIN lens has been manufactured and vibrometry measurements done to measure the transverse velocity on a plate equipped with the lens for different frequencies confirm the existence of a similar focal point where wave energy is concentrated. The proposed design is interesting as the focusing properties do not depend on the frequency, and the very simplified configuration based on the bounding of segments seriously reduces the fabrication complexity compared to continuous profiles. This paves the way for simpler focusing device integration strategies for vibroacoustic control or energy harvesting for instance.

Supplementary material

Videos presenting the wave propagation obtained numerically and experimentally in the plate with the GRIN lens composed of 7 segments are availabe as a supplementary material : DOI - 10.5281/zenodo.3933920). Three frequencies are considered (2350 Hz, 5300 Hz and 7900 Hz), and these results correspond to those in Fig. 10, 11 and 12.

Acknowledgements

This work has been supported by the EUR EIPHI Project (contract ANR-17-EURE-0002) and Bourgogne Franche-Comté Region. Authors want to thank the C.F.A.I from Besançon and in particular Simon Huot for their precious help in the manufacture of the lens elements.

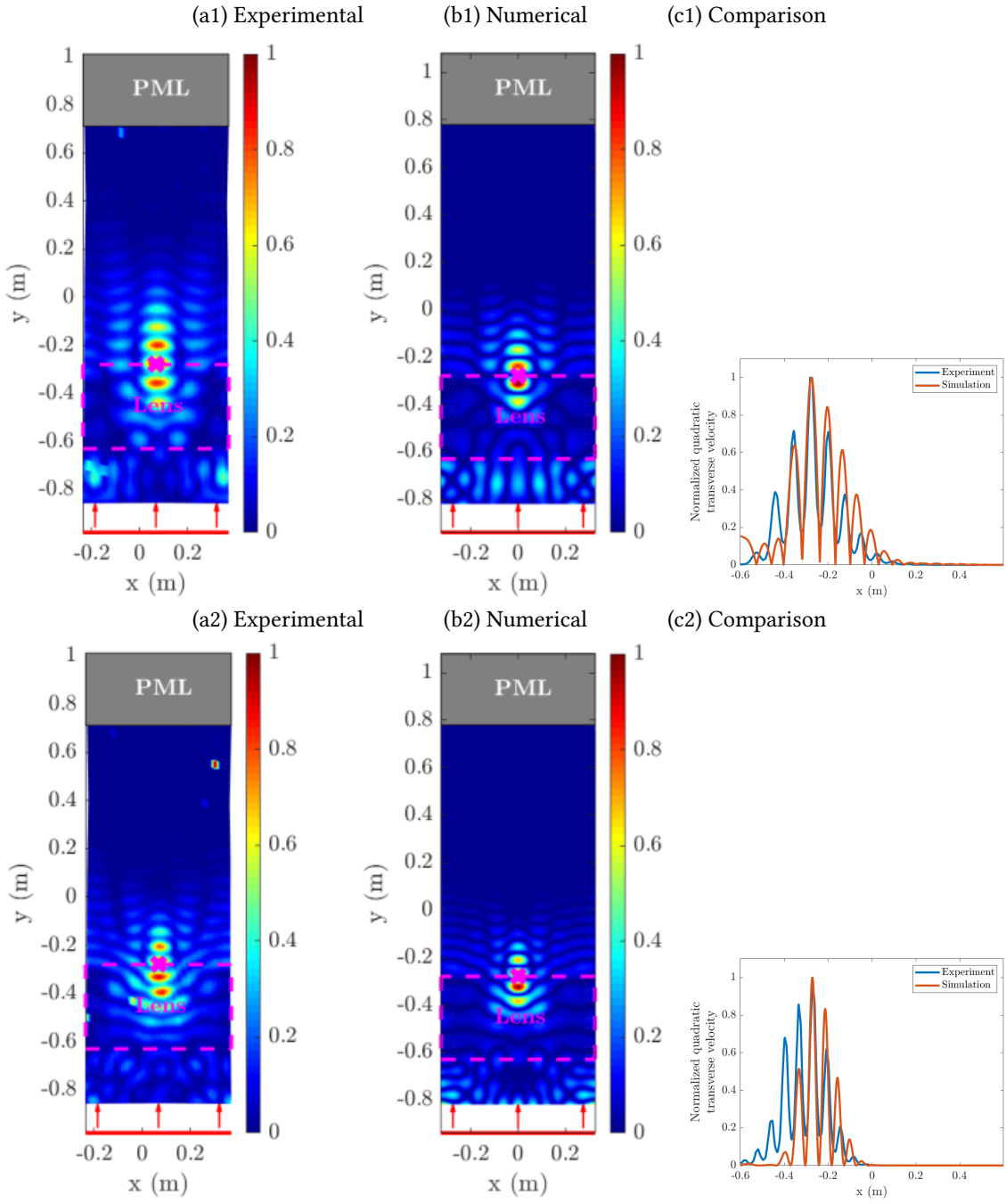

Figure 10: Nondimensionalized transverse velocity amplitude for a GRIN discrete lens : (a) Experimental results, (b) Simulation results, (c) Comparison of the quadratic velocity between experimental and numerical results along the central line in the direction of wave propagation - Case 1: f=2350 Hz, Case 2 : f=3450 Hz

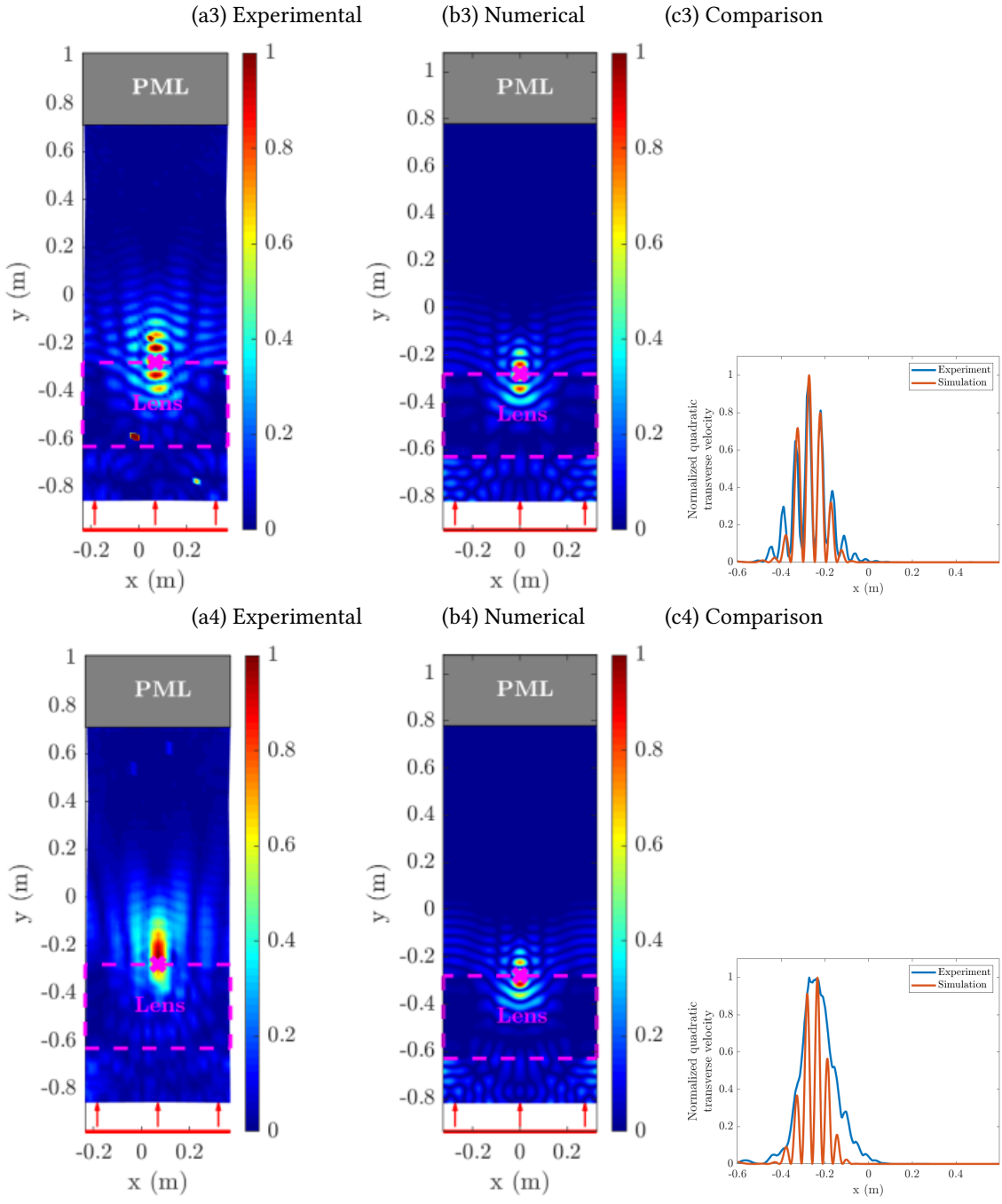

Figure 11: Nondimensionalized transverse velocity amplitude for a GRIN discrete lens : (a) Experimental results, (b) Simulation results, (c) Comparison of the quadratic velocity between experimental and numerical results along the central line in the direction of wave propagation - Case 3 : f=4400 Hz, Case 4 : f=5300 Hz

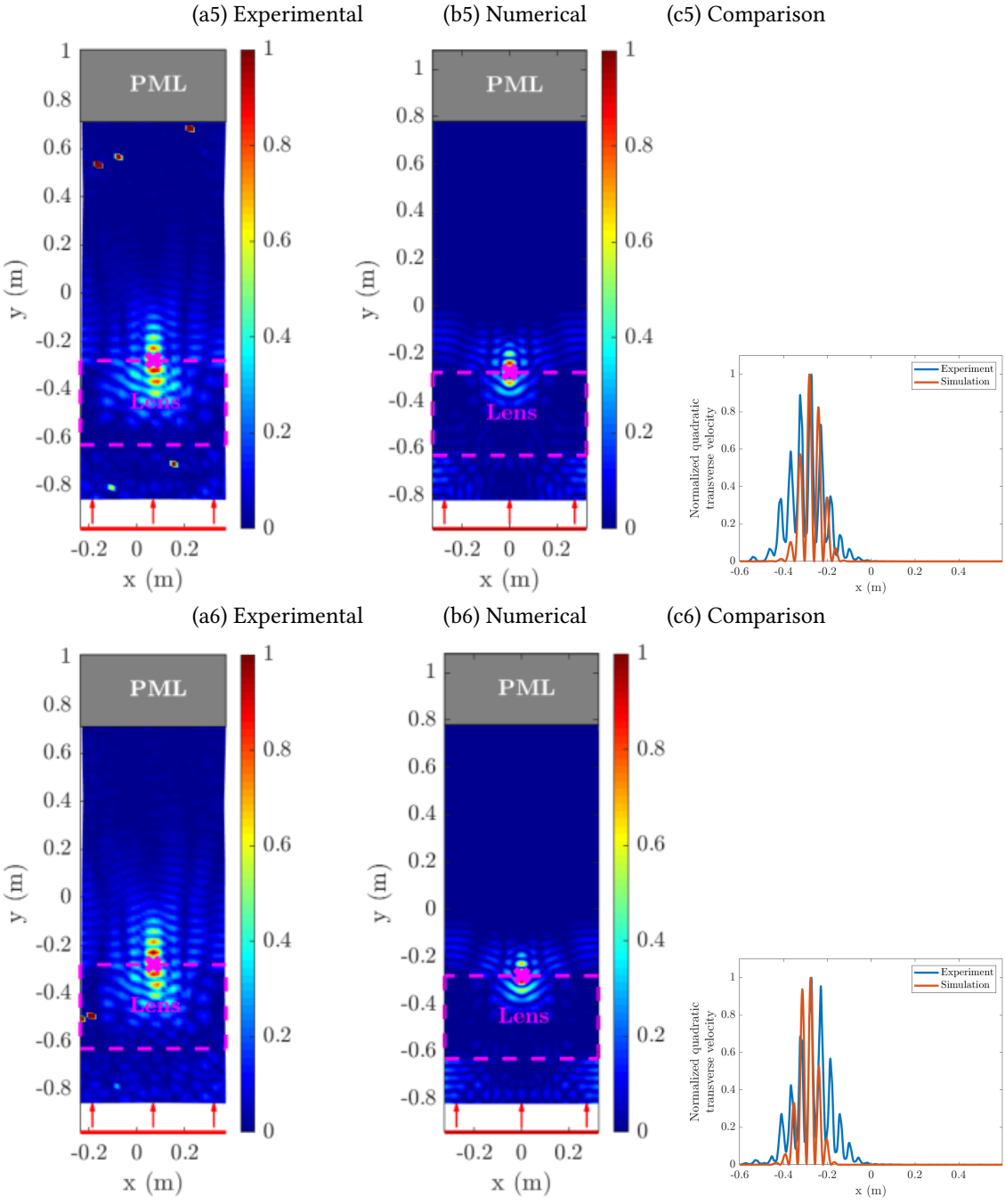

Figure 12: Nondimensionalized transverse velocity amplitude for a GRIN discrete lens : (a) Experimental results, (b) Simulation results, (c) Comparison of the quadratic velocity between experimental and numerical results along the central line in the direction of wave propagation -Case 5 : f=6850 Hz, Case 6 : f = 7900 Hz

References

Billon, K., Ouisse, M., Sadoulet-Reboul, E., Collet, M., Butaud, P., Chevallier, G. and Khelif, A. (2019), 'Design and experimental validation of a temperature-driven adaptive phononic crystal slab', *Smart Materials and Structures* **28**(3), 035007.

Campana, M., Ouisse, M., Sadoulet-Reboul, E., Ruzzene, M., Neild, S. and Scarpa, F. (2020), 'Impact of non-linear resonators in periodic structures using a perturbation approach', *Mechanical Systems and Signal Processing* **135**, 106408.

Carrara, M., Cacan, M., Leamy, M., Ruzzene, M. and Erturk, A. (2012), 'Dramatic enhancement of structure-borne wave energy harvesting using an elliptical acoustic mirror', *Applied Physics Letters* **100**(20), 204105.

Carrara, M., Cacan, M., Toussaint, J., Leamy, M., Ruzzene, M. and Erturk, A. (2013), 'Metamaterial-inspired structures and concepts for elastoacoustic wave energy harvesting', *Smart Materials and Structures* **22**(6), 065004.

Carrara, M., Kulpe, J., Leadenham, S., Leamy, M. and Erturk, A. (2015), 'Fourier transform-based design of a patterned piezoelectric energy harvester integrated with an elastoacoustic mirror', *Applied Physics Letters* **106**(1), 013907.

Centeno, E. and Cassagne, D. (2005), 'Graded photonic crystals', *Optics letters* **30**(17), 2278–2280.

Chiou, M.-J., Lin, Y.-C., Ono, T., Esashi, M., Yeh, S.-L. and Wu, T.-T. (2014), 'Focusing and waveguiding of lamb waves in micro-fabricated piezoelectric phononic plates', *Ultrasonics* **54**(7), 1984–1990.

Climente, A., Torrent, D. and Sánchez-Dehesa, J. (2014), 'Gradient index lenses for flexural waves based on thickness variations', *Applied Physics Letters* **105**(6), 064101.

Davis, M. R., Greegor, R. B., Li, K., Nielsen, J. A., Parazzoli, C. G. and Tanielian, M. H. (2007), 'Metamaterial scanning lens antenna systems and methods'. US Patent 7,218,285.

Deng, K., Ding, Y., He, Z., Zhao, H., Shi, J. and Liu, Z. (2009), 'Graded negative index lens with designable focal length by phononic crystal', *Journal of Physics D: Applied Physics* **42**(18), 185505.

Georgiev, V., Cuenca, J., Gautier, F., Simon, L. and Krylov, V. (2011), 'Damping of structural vibrations in beams and elliptical plates using the acoustic black hole effect', *Journal of sound and vibration* **330**(11), 2497–2508.

Gomez-Reino, C., Perez, M. V. and Bao, C. (2012), *Gradient-index optics: fundamentals and applications*, Springer Science & Business Media.

Hyun, J., Choi, W. and Kim, M. (2019), 'Gradient-index phononic crystals for highly dense flexural energy harvesting', *Applied Physics Letters* **115**(17), 173901.

Jin, Y., Torrent, D., Pennec, Y., Pan, Y. and Djafari-Rouhani, B. (2015), 'Simultaneous control of the s 0 and a 0 lamb modes by graded phononic crystal plates', *Journal of Applied Physics* **117**(24), 244904.

Krylov, V. and Tilman, F. (2004), 'Acoustic 'black holes' for flexural waves as effective vibration dampers', *Journal of Sound and Vibration* **274**(3-5), 605–619.

Kudela, P., Radzienski, M., Ostachowicz, W. and Yang, Z. (2018), 'Structural health monitoring system based on a concept of lamb wave focusing by the piezoelectric array', *Mechanical Systems and Signal Processing* **108**, 21–32.

Kurt, H., Colak, E., Cakmak, O., Caglayan, H. and Ozbay, E. (2008), 'The focusing effect of graded index photonic crystals', *Applied Physics Letters* **93**(17), 171108.

Lin, S.-C. S., Huang, T. J., Sun, J.-H. and Wu, T.-T. (2009), 'Gradient-index phononic crystals', *Physical Review B* **79**(9), 094302.

Peng, S., He, Z., Jia, H., Zhang, A., Qiu, C., Ke, M. and Liu, Z. (2010), 'Acoustic far-field focusing effect for two-dimensional graded negative refractive-index sonic crystals', *Applied Physics Letters* **96**(26), 263502.

Sukhovich, A., Jing, L. and Page, J. H. (2008), 'Negative refraction and focusing of ultrasound in two-dimensional phononic crystals', *Physical Review B* **77**(1), 014301.

Timorian, S., Ouisse, M., Bouhaddi, N., De Rosa, S. and Franco, F. (2020), 'Numerical investigations and experimental measurements on the structural dynamic behaviour of quasi-periodic meta-materials', *Mechanical Systems and Signal Processing* **136**, 106516.

Tol, S., Degertekin, F. and Erturk, A. (2016), 'Gradient-index phononic crystal lens-based enhancement of elastic wave energy harvesting', *Applied Physics Letters* **109**(6), 063902.

Tol, S., Degertekin, F. and Erturk, A. (2017), 'Structurally embedded reflectors and mirrors for elastic wave focusing and energy harvesting', *Journal of Applied Physics* **122**(16), 164503.

Tol, S., Degertekin, F. and Erturk, A. (2019), '3d-printed phononic crystal lens for elastic wave focusing and energy harvesting', *Additive Manufacturing* **29**, 100780.

Wu, T.-T., Chen, Y.-T., Sun, J.-H., Lin, S.-C. S. and Huang, T. J. (2011), 'Focusing of the lowest antisymmetric lamb wave in a gradient-index phononic crystal plate', *Applied Physics Letters* **98**(17), 171911.

Xu, J., Li, S. and Tang, J. (2017), Adaptive grin lens based on piezoelectric metamaterial for acoustic beam focusing, *in* 'Active and Passive Smart Structures and Integrated Systems 2017', Vol. 10164, International Society for Optics and Photonics, p. 101641S.

Yan, X., Zhu, R., Huang, G. and Yuan, F. (2013), Focusing flexural lamb waves by designing elastic metamaterials bonded on a plate, *in* 'Health Monitoring of Structural and Biological Systems 2013', Vol. 8695, International Society for Optics and Photonics, p. 86952P.

Yi, K., Collet, M., Ichchou, M. and Li, L. (2016), 'Flexural waves focusing through shunted piezoelectric patches', *Smart Materials and Structures* **25**(7), 075007.

Yi, K., Ouisse, M., Sadoulet-Reboul, E. and Matten, G. (2019), 'Active metamaterials with broadband controllable stiffness for tunable band gaps and non-reciprocal wave propagation', *Smart Materials and Structures* **28**(6), 065025.

Zareei, A., Darabi, A., Leamy, M. J. and Alam, M.-R. (2018), 'Continuous profile flexural grin lens: Focusing and harvesting flexural waves', *Applied Physics Letters* **112**(2), 023901.

Zhao, J., Marchal, R., Bonello, B. and Boyko, O. (2012), 'Efficient focalization of antisymmetric lamb waves in gradient-index phononic crystal plates', *Applied Physics Letters* **101**(26), 261905.

Zhu, H. and Semperlotti, F. (2017), 'Two-dimensional structure-embedded acoustic lenses based on periodic acoustic black holes', *Journal of Applied Physics* **122**(6), 065104.

A Parameters

The table 2 contains all the geometrical and material parameters used for the numerical simulations.

Parameter	Variable [Unit]	Value
Parameters for the plate		
L	Length [m]	1.9
w	width [m]	0.065
h_0	thickness [m]	0.005
E	Young's modulus [GPa]	70
ρ	density [kg.m^{-3}]	2700
ν	Poisson's ratio	0.3
Parameters for the piezoelectric patches		
l_p	length [m]	0.03
w_p	width [m]	0.03
h_p	thickness [m]	0.005
ρ_p	density [kg.m^{-3}]	7760
$\epsilon_1^\sigma = \epsilon_2^\sigma$, ϵ_3^σ	dielectric permittivity	1936 ϵ_0, 2109 ϵ_0
Compliance matrix under constant electric field		
$S_{11}^E = S_{22}^E$, S_{33}^E	[Pa^{-1}]	1.683x10^{-11}, 1.9x10^{-11}
S_{12}^E, $S_{13}^E = S_{23}^E$	[Pa^{-1}]	-5.656x10^{-12}, -7.707x10^{-12}
$S_{44}^E = S_{55}^E$, S_{66}^E	[Pa^{-1}]	5.096x10^{-11}, 4.497x10^{-11}
Piezoelectric matrix		
$d_{31} = d_{32}$	[C/N]	-2.14x10^{-10}
d_{33}	[C/N]	4.230x10^{-10}
$d_{24} = d_{15}$	[C/N]	6.1x10^{-10}
Parameters for the PML		
l_{pml}	length [m]	0.3
w_{pml}	width [m]	0.65 = w
h_{pml}	thickness [m]	0.005 = w

Table 2: Parameters for the numerical simulations